Deletions Involving Long-Range Conserved Nongenic Sequences Upstream and Downstream of *FOXL2* as a Novel Disease-Causing Mechanism in Blepharophimosis Syndrome

D. Beysen,[1] J. Raes,[3] B. P. Leroy,[1,2] A. Lucassen,[4] J. R. W. Yates,[5] J. Clayton-Smith,[6] H. Ilyina,[7] S. Sklower Brooks,[8] S. Christin-Maitre,[9] M. Fellous,[10] J. P. Fryns,[11] J. R. Kim,[12] P. Lapunzina,[13] E. Lemyre,[14] F. Meire,[3] L. M. Messiaen,[15] C. Oley,[16] M. Splitt,[17] J. Thomson,[18] Y. Van de Peer,[3] R. A. Veitia,[10] A. De Paepe,[1] and E. De Baere[1]

[1]Center for Medical Genetics and [2]Department of Ophthalmology, Ghent University Hospital, and [3]Research Group of Bioinformatics and Evolutionary Genomics, Department of Plant Systems Biology, Ghent University–Flemish Institute for Biotechnology, Ghent, Belgium; [4]Wessex Clinical Genetics Service, University of Southampton, Southampton, United Kingdom; [5]Department of Medical Genetics, University of Cambridge and Addenbrooke's Hospital, Cambridge, United Kingdom; [6]Academic Department of Medical Genetics, St. Mary's Hospital, Manchester, United Kingdom; [7]Belorussian Institute for Hereditary Disorders, Minsk, Belarus; [8]New York State Institute for Basic Research in Developmental Disabilities, New York; [9]Service d'Endocrinologie, Hôpital Saint-Antoine, and [10]INSERM U361 Reproduction et Physiopathologie Obstétricale Hôpital Cochin, Paris; [11]Center for Human Genetics, Leuven, Belgium; [12]Department of Biochemistry and Molecular Biology, Yeungnam University, Daegu, Republic of Korea; [13]Servicio de Genética, Hospital Universitario La Paz, Madrid; [14]Medical Genetics Service, Department of Pediatrics, Hôpital Sainte-Justine, Université de Montréal, Montreal; [15]University of Alabama, Birmingham; [16]Birmingham Women's Hospital, Birmingham, United Kingdom; [17]Department of Clinical Genetics, Guy's and St Thomas' Hospital National Health Service Trust, London; and [18]Clinical Genetics, St. James's University Hospital, Leeds, United Kingdom

The expression of a gene requires not only a normal coding sequence but also intact regulatory regions, which can be located at large distances from the target genes, as demonstrated for an increasing number of developmental genes. In previous mutation studies of the role of *FOXL2* in blepharophimosis syndrome (BPES), we identified intragenic mutations in 70% of our patients. Three translocation breakpoints upstream of *FOXL2* in patients with BPES suggested a position effect. Here, we identified novel microdeletions outside of *FOXL2* in cases of sporadic and familial BPES. Specifically, four rearrangements, with an overlap of 126 kb, are located 230 kb upstream of *FOXL2*, telomeric to the reported translocation breakpoints. Moreover, the shortest region of deletion overlap (SRO) contains several conserved nongenic sequences (CNGs) harboring putative transcription-factor binding sites and representing potential long-range *cis*-regulatory elements. Interestingly, the human region orthologous to the 12-kb sequence deleted in the polled intersex syndrome in goat, which is an animal model for BPES, is contained in this SRO, providing evidence of human-goat conservation of *FOXL2* expression and of the mutational mechanism. Surprisingly, in a fifth family with BPES, one rearrangement was found downstream of *FOXL2*. In addition, we report nine novel rearrangements encompassing *FOXL2* that range from partial gene deletions to submicroscopic deletions. Overall, genomic rearrangements encompassing or outside of *FOXL2* account for 16% of all molecular defects found in our families with BPES. In summary, this is the first report of extragenic deletions in BPES, providing further evidence of potential long-range *cis*-regulatory elements regulating *FOXL2* expression. It contributes to the enlarging group of developmental diseases caused by defective distant regulation of gene expression. Finally, we demonstrate that CNGs are candidate regions for genomic rearrangements in developmental genes.

Introduction

The expression pattern of many developmental genes is regulated at different levels. Usually, basal gene expression is controlled by the core promoter, located immediately upstream of the ORF. However, spatiotemporally and quantitatively correct gene expression is often controlled by long-range *cis*-acting regulatory elements as distant as 1.1 Mb (Velagaleti et al. 2005). These elements (enhancers, insulators, and locus-control regions) can be located upstream or downstream of the transcription unit of a gene. Interspecies comparative studies show a strong evolutionary conservation of these elements, which may reside in unrelated neighboring genes or intergenic regions. Genomic rearrangements involving such elements outside of a transcription unit can give rise to human disease by a dissociation of the transcrip-

Received April 22, 2005; accepted for publication May 19, 2005; electronically published June 16, 2005.

Address for correspondence and reprints: Dr. Elfride De Baere, Center for Medical Genetics, Ghent University Hospital, De Pintelaan 185, B-9000 Ghent, Belgium. E-mail: Elfride.DeBaere@UGent.be

0002-9297/2005/7702-0004$15.00

tion unit and its *cis*-acting regulatory elements, by an alteration of the chromatin structure, or by both mechanisms (reviewed by Kleinjan and van Heyningen [2005]).

Recently, it was shown that heterozygous mutations of the *FOXL2* gene (MIM 605597), which encodes a forkhead transcription factor, cause both types of blepharophimosis-ptosis-epicanthus inversus syndrome (BPES [MIM 110100]). BPES is a rare, autosomal dominant developmental disorder characterized by an eyelid malformation. Two subtypes have been identified; type I is associated with premature ovarian failure (POF), whereas type II is not (Zlotogora et al. 1983). It was shown that haploinsufficiency of *FOXL2* was caused by intragenic mutations, in most cases, and by submicroscopic deletions encompassing *FOXL2* and neighboring genes, in two cases (De Baere et al. 2001, 2003). A genotype-phenotype correlation was proposed mainly on the basis of intragenic mutations distinguishing the two BPES types at the molecular level (De Baere et al. 2003). Despite the ovarian phenotype in BPES, several studies have indicated that mutations in *FOXL2* do not play a major role in causing idiopathic POF (De Baere et al. 2001, 2002; Harris et al. 2002; Bodega et al. 2004).

A spatiotemporally restricted expression pattern of the *FOXL2* transcript and protein was demonstrated in several species (human, mouse, and goat). It was shown to be expressed in developing eyelids and in granulosa cells of fetal and adult ovaries (Crisponi et al. 2001; Cocquet et al. 2002, 2003). Recently, two studies presenting homozygous knockout mice showed that granulosa cell function is crucial not only for oocyte growth but also for ovarian maintenance, thus providing a molecular mechanism for POF in BPES in vivo (Schmidt et al. 2004; Uda et al. 2004).

During the positional cloning of *FOXL2,* three balanced translocations were characterized in patients with a classic BPES phenotype. It was shown that the breakpoints of these translocations disrupt two other genes (*BPESC1* and *MRPS22*), both devoid of pathogenic mutations in other patients with BPES, suggesting a position effect (De Baere et al. 2000; Praphanphoj et al. 2000; Crisponi et al. 2001, 2004).

Sequencing of the *FOXL2* ORF, in combination with FISH analysis with a probe encompassing the *FOXL2* gene, revealed mutations in <70% of patients with BPES (De Baere et al. 2001, 2003). Here, we applied a novel mutation-detection strategy consisting of multiplex ligation-dependent probe amplification (MLPA), genotyping with >60 microsatellites and SNPs, and comprehensive FISH analysis. This approach led to the identification of nine novel deletions encompassing *FOXL2,* which ranged from partial and total gene deletions to microdeletions and submicroscopic deletions. Notably, five novel deletions were found either upstream or downstream of the transcription unit of *FOXL2.* These genic and extragenic (micro)deletions account for 11% and 5%, respectively, of all molecular defects found in our cohort with BPES. Finally, we report the first case of germline mosaicism in a family with BPES that is confirmed at the molecular level.

Material and Methods

Patients and Diagnostic Criteria

The 37 consenting probands with BPES who were included in this study presented with blepharophimosis, ptosis, epicanthus inversus, and telecanthus. The clinical diagnosis was given by a clinical geneticist or an ophthalmologist. When possible, karyotyping was performed in the referring laboratory. The karyotype was not confirmed by us. In each proband, intragenic mutations were excluded by sequencing of the *FOXL2* ORF, as described by De Baere et al. (2001).

Custom-Made MLPA

MLPA permits relative quantification of changes in copy number of specific chromosomal sequences (Schouten et al. 2002). A custom-made deletion-detection kit for *FOXL2* was developed by MRC-Holland (P054 *FOXL2*) and contains three different probes for *FOXL2* (FOXL2-D01, FOXL2-D02, and FOXL2-D03), four probes for the *ATR* gene (located at 3q22-24), and probes for other genes (*TWIST, FOXC1, PITX2, FOXC2,* and *OA1*). Probe FOXL2-D01 is located in the forkhead domain (c.252–351; g.489–588), probe FOXL2-D02 is between the forkhead domain and the polyalanine tract (c.575–641; g.812–878), and probe FOXL2-D03 is downstream of the polyalanine tract (c.1053–1113; g.1290–1350). MLPA was performed in accordance with the manufacturer's instructions.

FISH

A genomic BAC contig of region 3q23 was obtained from the National Center for Biotechnology Information (NCBI) database. BACs were obtained from The Wellcome Trust Sanger Institute and BACPAC Resources Center. PACs and cosmids had been previously obtained from the UK–Medical Research Council and were mapped by FISH (De Baere et al. 1999). BAC, PAC, and cosmid DNA was prepared and labeled with the use of standard conditions. FISH analysis was performed as described by De Baere et al. (1999).

Microsatellite Analysis

Fifteen polymorphic microsatellites (with prefix "D3S") were selected from the NCBI on the basis of location and heterozygosity. Primer sequences of markers with

Table 1

Primer Sequences of Novel Microsatellites and SNaPshot Analysis

The table is available in its entirety in the online edition of *The American Journal of Human Genetics*.

prefixes "VY" and "NU" were obtained from Udar et al. (2003). A third series of microsatellites (Tel2 and markers with prefix "EDB") was developed by a manual search for repeats in the BAC sequences derived from NCBI. For a fourth series (with prefix "DB"), the different BAC sequences were analyzed using the Find Simple Repeats software, which selects repetitive sequences that are expected to have a very high degree of polymorphism. The search was confined to sequences presenting repetitions with a maximum of 4 nt and having a total length of at least 12 nt. Sequences with a score $\geqslant$30 were selected for primer design. Primer sequences are given in table 1. Characterization of the polymorphic nature of the known and novel microsatellites was performed in a white population by use of an M13-system described by Schuelke (2000). For allele sizing, aliquots of PCR reaction were mixed with ROX-500 or ROX-1000 size standard (Applied Biosystems) and formamide and were separated on an ABI PRISM 3100 Genetic Analyzer (Applied Biosystems). Fragment sizing was performed automatically using GeneScan version 3.7. The different microsatellite alleles were numbered consecutively, in order of increasing size. The numbering is different for each family.

SNaPshot Analysis

Twenty-seven SNP loci were selected from the International HapMap Project database, and amplification primers were designed so that PCR products of ~300 bp were obtained. Typing primers were designed to anneal to the target DNA flanking the 3′ end of the SNP. A standard PCR reaction was performed, followed by exonuclease I and shrimp alkaline phosphatase (SAP) treatment (Amersham). A single-nucleotide primer extension reaction was performed using an ABI PRISM SNaPshot Multiplex kit (Applied Biosystems), in accordance with the manufacturer's instructions. After SAP treatment, products were separated on an ABI PRISM 3100 Genetic Analyzer (Applied Biosystems) and were analyzed with GeneScan version 3.7. Numbers were assigned to alleles as follows: A = 1, C = 2, G = 3, and T = 4.

To assess the degree of germline mosaicism in an unaffected male, quantitative SNaPshot analysis was performed as described by Mátyás et al. (2002). For normalization, genomic samples from four unrelated individuals who have an identical SNP haplotype as that of the test sample were used as controls.

Long-Range PCR

For long-range PCR, the Expand Long Template PCR System (Roche) was used. A master mix of 50 μl contained 300 ng of genomic DNA, 0.5 μM of each primer, 5 μl of Expand Long Template PCR buffer 3 (containing 10 × PCR buffer and 27.5 mM $MgCl_2$), 3.75 U of Expand Long Template enzyme mix (containing *Taq* DNA polymerase and *Tgo* DNA polymerase), 500 μM of each dNTP, and 3 mM additional $MgCl_2$. Cycling conditions included an initial denaturation cycle at 94°C for 2 min, followed by 10 cycles at 94°C for 20 s, 65°C for 30 s, and 68°C for 12 min; 25 cycles at 94°C for 30 s and 65°C for 30 s and elongation for 12 min plus 20 s for each successive cycle; and a final extension at 72°C for 7 min.

Construction of a High-Resolution Physical Map Covering Microdeletions

First, we generated a sequence contig of 16 overlapping RPCI-11 BAC clones that span ~1.8 Mb surrounding *FOXL2* by a search of GenBank (NCBI). The polymorphic microsatellites selected from NCBI were positioned on this BAC contig by use of the reference numbering of build 34, version 3 ("the golden path"), and by use of BLAST (NCBI). The localization of the anonymous microsatellites and SNPs was verified by BLAST searches against the BAC sequences. The exact PAC and cosmid localization was determined by BLAST after PAC and cosmid end sequencing, in accordance with standard protocol. Finally, the different known and unassigned genes that are located in this region were added to the map according to NCBI data.

Comparative Sequence Analysis

To identify conserved nongenic sequences (CNGs), comparative sequence analysis of the regions of interest was performed using the University of California–Santa Cruz (UCSC) Genome Browser. The UCSC Multiz Alignments and Conservation track contains a measure of evolutionary conservation in human, chimp, mouse, rat, dog, chicken, pufferfish, and zebrafish based on a phylogenetic hidden Markov model (phastCons). The overall conservation score across all species, as well as pairwise alignments of each species aligned to the human genome, were retrieved, and gapped alignments were included. The length of the alignment is based on the lengths of gaps in the human sequence at those alignment positions, relative to the longest nonhuman sequence. Alignments are based on the following genome assemblies: human, May 2004 (hg17); chimp, November 2003 (panTro1); mouse, May 2004 (mm5); rat, June 2003 (rn3); dog, July 2004 (canFam1); chicken, February 2004 (galGal2); *Fugu,* August 2002 (fr1); and zebrafish,

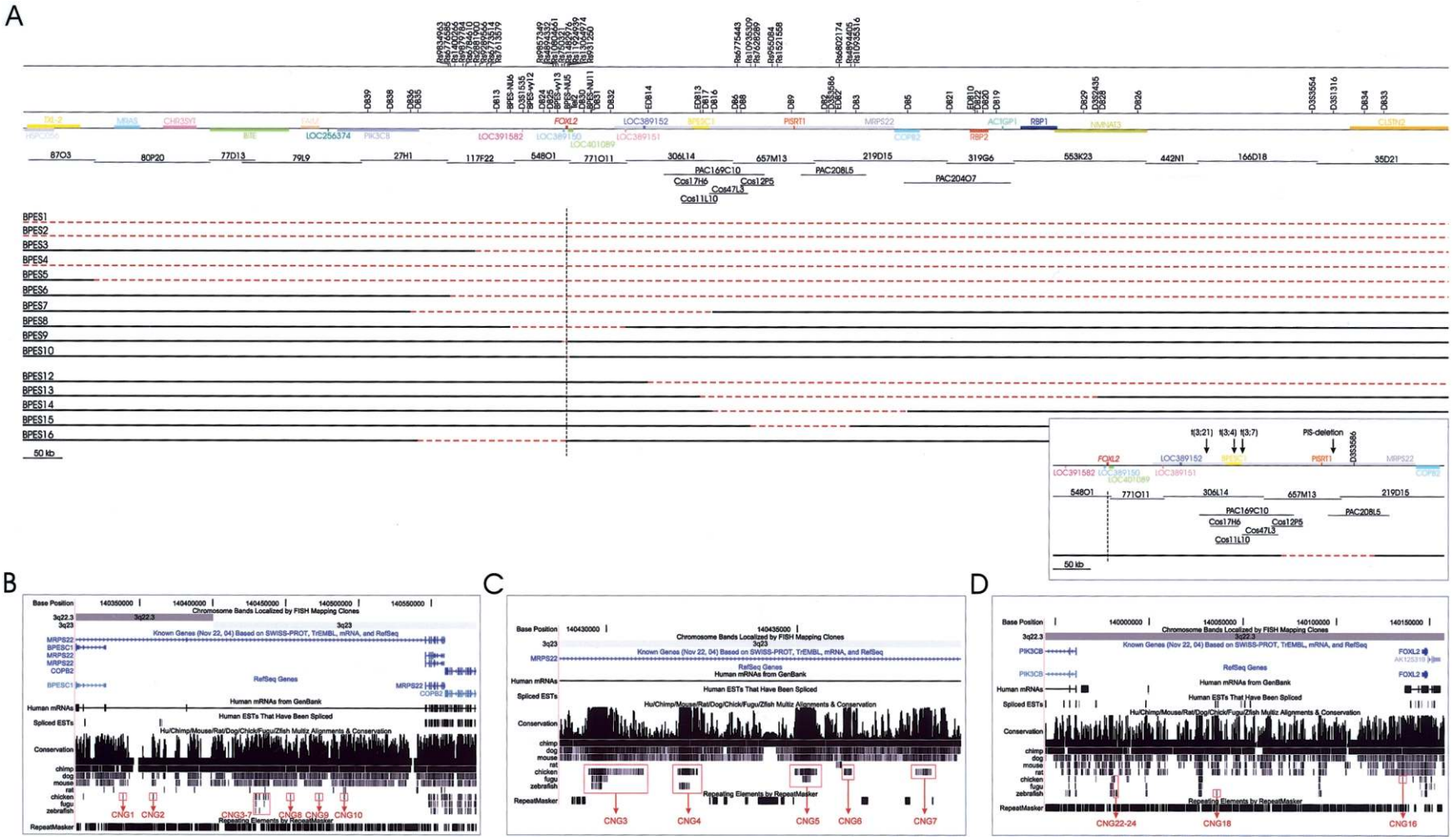
A
FOXL2
LOC389152
PISRT1
MRPS22
LOC391582
LOC389150
LOC389151
LOC401089
PIK3CB
LOC256374
BPES1
BPES2
BPES3
BPES4
BPES5
BPES6
BPES7
BPES8
BPES9
BPES10
BPES12
BPES13
BPES14
BPES15
BPES16
50 kb
PAC169C10
Cos17H6
Cos12P5
Cos47L3
Cos11L10
PAC208L5
PAC204O7
t(3;21)
t(3;4)
t(3;7)
PIS-deletion
B
C
D
CNG1
CNG2
CNG3-7
CNG8
CNG9
CNG10
CNG3
CNG4
CNG5
CNG6
CNG7
CNG22-24
CNG18
CNG16

November 2003 (danRer1). Our selection criteria included conservation at least up to chicken, pufferfish, and/or zebrafish, independent of alignment length, percentage of conservation, and presence of gaps.

The respective sequences of the selected elements and their corresponding mouse sequences were retrieved through the UCSC Genome Browser. Apart from these sequences, an available 48-kb goat sequence from the polled intersex syndrome (PIS) locus (GenBank accession number AF404302) was retrieved for human-goat comparison with the use of mVista. A pairwise alignment was performed between human and mouse, human and goat, human and chicken, human and pufferfish, and human and zebrafish by use of ClustalW. To exclude the coding potential of all putative CNGs, the human sequence of the conserved region was compared with all available EST and protein sequences in GenBank, as well as with all gene predictions for the selected region available from the UCSC Genome Browser and the Biomax Human Genome Database (blastn, blastx, tblastx, and nrprot). In addition, sequences were scanned for repetitive elements using RepeatMasker. Sequences that did not show significant similarity to known proteins, genes and/or transcripts, or transposable elements were selected as CNGs. These were searched against the Transfac database (version 8.3) of known vertebrate *cis*-acting regulatory DNA elements and *trans*-acting factors by use of the Match tool included in that database (Matys et al. 2003). Only highly significant matches with transcription-factor binding sites were considered, by use of the built-in "minimize false positive matches" setting.

Results and Discussion

The mutation detection rate of <70% in previous mutation studies of *FOXL2* in BPES could be explained by clinical misdiagnosis; the sensitivity of the strategy used, which might not allow detection of changes in gene copy number or in distant sequences outside of the transcription unit of *FOXL2* (De Baere et al. 2001, 2003); or the presence of a second BPES locus, although there is no evidence to support the existence of a second locus. Here, we developed a novel combined approach consisting of (1) custom-made MLPA for detection of changes in gene copy number of *FOXL2* and other genes; (2) a genotyping panel, comprising 15 known and 32 anonymous microsatellites and 26 SNPs; and (3) comprehensive FISH analysis whenever possible.

Genomic Rearrangements Encompassing FOXL2

A clue to subtle *FOXL2* deletions was found in similar observations for *FOXC1*, which encodes a forkhead transcription factor associated with ocular anterior segment dysgenesis (IRID1 [MIM 601631]). Irrespective of whether the gene is duplicated or deleted, a nearly identical ocular phenotype is observed, showing that exact gene dosage of *FOXC1* is critical for normal eye development (Lehmann et al. 2003).

Our approach allowed identification of 11 deletions encompassing *FOXL2,* of which 9 are novel. These deletions contribute to 11% (11/100) of all molecular defects found in our series of patients with BPES and are found in 30% (11/37) of mutation-negative patients. They occur in sporadic cases and familial cases and are absent in all unaffected family members analyzed. A graphical overview of these deletions is given in figure 1*A*. Clinical data for the 11 families and molecular details on the deletions are summarized in table 2.

The rearrangements include one partial *FOXL2* deletion (in BPES10), an 8-kb deletion removing the whole *FOXL2* ORF (in BPES9), two microdeletions of up to 420 kb, encompassing *FOXL2* and neighboring genes (in BPES7 and BPES8), four submicroscopic deletions (in BPES2, BPES4, BPES5, and BPES6), and two micro-

Figure 1 *A,* Physical map of a 1.8-Mb region flanking *FOXL2* that shows the position of the BACs, PACs, cosmids, microsatellites, and SNPs that were used for identification and delineation of the deletions. The map is drawn to scale; the size equivalent to 50 kb is given at the bottom left corner. The location of *FOXL2* is indicated by a vertical black line. The top line represents the localization of SNPs, and the second line contains the known and anonymous microsatellites used in this study. In the third line, the location of the genes in this region is shown, whereas the BACs, PACs, and cosmids used for FISH are shown below the line. The lower part of *A* is an overview of all deletions identified in this study, except one. Every line represents a patient or family in whom a deletion was found. The dashed red line shows the maximal extent of the deletion. The first 10 lines represent the deletions that encompass *FOXL2*. The deletion identified in BPES11 is not shown, since the extent of the deletion could not be determined because of a lack of material for FISH and microsatellite analysis. The second group represents the five extragenic deletions (four upstream and one downstream). Clinical details and molecular data on the patients with deletions are shown in table 2. In a box at the bottom right, a detailed view of the SRO of the four upstream extragenic deletions is shown. The position of *FOXL2* is marked by a vertical dashed black line, and the SRO is shown by the dashed red line. The positions of the known three translocation breakpoints at 3q23 in BPES and of the orthologue of the PIS locus are indicated by vertical arrows. *B* and *C,* UCSC Genome Browser map of the SRO of the four upstream extragenic rearrangements in families BPES12, BPES13, BPES14, and BPES15. CNGs are highlighted at the bottom with red boxes. Their names, based on our arbitrary numbering, are given below the boxes. Details on all CNGs can be found in table 4. The CNGs shown in *B* are evolutionarily conserved up to chicken. *C* represents a more detailed view of CNG3–CNG7. CNG3–CNG5 are conserved up to zebrafish and/or pufferfish. They all represent potential *cis*-regulatory elements of the *FOXL2* region. *D,* UCSC Genome Browser map of the sequence contained in the downstream extragenic rearrangement in family BPES16. Five CNGs are indicated in this 3′ SRO, of which several are conserved up to zebrafish and/or pufferfish (CNG14, CNG18, and CNG22–CNG24).

Table 2

Summary of Clinical and Molecular Findings in Patients with BPES Who Have Deletions Encompassing *FOXL2* or Outside of the Transcription Unit of *FOXL2*

Type of Genomic Rearrangement and Family	Type of BPES[a]	Origin[b]	Clinical Data[c]	Type of Deletion[d]	Karyotype	MLPA Finding[d]	Extent of Deletion[d]	Delineation of Centromeric Breakpoint[e]	Delineation of Telomeric Breakpoint[e]	Confirmed by FISH	Parental Origin
Encompassing *FOXL2*:											
BPES1	F2	KR	6-y-old male with psychomotor retardation and VSD (Cha et al. 2003)	Microscopic del incl. *FOXL2* in II:2	…	Total *FOXL2* and *ATR* del	>6.1 Mb in II:2 (137606245–143780323)	*D3S1238–D3S3528* (2.20 Mb)	Telomeric to *ATR*	No	Maternal
BPES2	S	NO	11-y-old male with psychomotor retardation, widely spaced nipples, scoliosis, high arched palate, and umbilical hernia (De Baere et al. 2003)	Submicroscopic del incl. *FOXL2*	Normal	Total *FOXL2* and *ATR* del	>3.8 Mb (139895393–143780323)	*D3S3617–DB39* (1.81 Mb)	Telomeric to *ATR*	Yes	Maternal
BPES3	S	GB	4-y-old female with postnatal growth retardation and microcephaly	Microscopic del incl. *FOXL2*	46,XX,del(3) (q22q23)	Total *FOXL2* del (3 probes); *ATR* normal	Max. 3.6 Mb (140031707–143650777)	*rs2881900–DB13* (26.99 kb)	*D3S1309–ATR* (1.44 Mb)	No	Maternal
BPES4	S	CA	3-y-old female with normal psychomotor development and no intrauterine and postnatal growth retardation; ultrasound of uterus and ovaries was normal at age 13 mo	Submicroscopic del incl. *FOXL2*	Normal	Total *FOXL2* del (3 probes); partial *ATR* del (1 probe)	>3.5 Mb (140058657–143651142)	*D3S3617–DB13* (1.97 Mb)	*ATR* gene	Yes	Maternal
BPES5	F	DK	II:1 had psychomotor and growth retardation and high arched palate; I:1 had growth retardation, with no clinical data about psychomotor development (De Baere et al. 2001)	Submicroscopic del incl. *FOXL2*	Normal	Total *FOXL2* del (3 probes)	Max. 3.2 Mb (139548627–142750847)	In BAC RP11-80P20 (147 kb)	*D3S3554–D3S3711* (1.66 Mb)	Yes	Unknown
BPES6	S	ES	1.5-y-old female with abnormal nose, normal psychomotor development, and no growth retardation; ultrasound of uterus and ovaries was normal	Submicroscopic del incl. *FOXL2*	Normal	Total *FOXL2* del (3 probes); *ATR* normal	Max. 2.7 Mb (140036995–142750847)	*rs9289566–rs6776585* (36.77 kb)	*D3S1309–D3S3711* (541.72 kb)	No	Paternal
BPES7	F	ES	Father and son with normal psychomotor development	Microdel incl. *FOXL2*	Normal	Total *FOXL2* del (3 probes)	Max. 412 kb (139949789–140359539)	*DB36–DB35* (9.4 kb)	*DB16–DB6* (28.21 kb)	Yes	Paternal?
BPES8	S	CD-BE	3-y-old female with normal psychomotor development	Microdel incl. *FOXL2*	…	Total *FOXL2* del (3 probes)	Max. 243 kb (140075997–140319005)	*NU6–D3S1535* (15.8 kb)	*DB 31–DB17* (45.11 kb)	Yes	Paternal
BPES9	F1	FR	II:1 had secondary amenorrhea; III:2 had heart malformation (mild interauricular communication)	Total *FOXL2* del	…	Total *FOXL2* del (3 probes)	8,226 nt (140141021–140149217)	In BAC RP11-548O1, nt 60868	BAC RP11-548O1, nt 69094	No	Unknown
BPES10	S	GB	4-y-old female with normal psychomotor development	Partial *FOXL2* del	Normal	Partial *FOXL2* del (2/3 probes)	Max. 6 kb (140147210–140150682)	In *FOXL2*, between MLPA probes 2 and 3 (416 nt)	*FOXL2*–Tel2 (2,440 nt)	No	Unknown
BPES11	S1	AU	36-y-old female with normal psychomotor development, menarche at age 18 y, only two periods, and very high FSH levels; IVF failed	(Micro)del incl. *FOXL2*	Normal	Total *FOXL2* del (3 probes)	…	…	…	No	Unknown

Outside transcription unit of *FOXL2*:											
BPES12	S	BY	15-y-old male with normal psychomotor development, intrauterine and postnatal growth retardation, microcephaly, ventricular septum defect, small mouth, contracture of interphalangeal joints, and right iris heterochromia	Microdel upstream of *FOXL2* (at 101 kb)	Normal	Two copies of *FOXL2* and *ATR* (*D3S1309* is heterozygous)	Max. 1.9 Mb (140249840–142209012)	*EDB14–DB17* (69.40 kb)	*DB33–D3S1309* (1.03 Mb)	No	Paternal
BPES13	S	PL	2-y-old female with stenosis of lacrimal duct, normal psychomotor development, microcephaly, and renal reflux	Microdel upstream of *FOXL2* (at 101 kb)	Normal	Two copies of *FOXL2*	Max. 567 kb (140249840–140816803)	*EDB14–DB16* (81.64 kb)	*DB19–D3S2435* (129.11 kb)	No	Maternal
BPES14	F2	GB	2-generation family. I:2 had astigmatism, three pregnancies, oligomenorrhea at age 40 y, and amenorrhea at age 47 y. II:1 had strabismus, normal menarche at age 12 y, and oligomenorrhea with elevated FSH and LH at age 38 y. Both I:2 and II:1 had normal growth and psychomotor development.	Microdel upstream of *FOXL2* (at 183 kb)	…	Two copies of *FOXL2* and *ATR*	Max. 244 kb (140331480–140575742)	*DB16–D3S3586* (144.53 kb)	*rs4894405–DB5* (71.90 kb)	Yes	Unknown
BPES15	F2	BE	5-generation family with typical BEPS. Affected members, normal psychomotor development	Microdel upstream of *FOXL2* (at 231 kb)	Normal	Two copies of *FOXL2*	Max. 126 kb (140377649–140503837)	*rs10935309–rs955084* (27.14 kb)	*rs6802174–rs4894405* (14.47 kb)	Yes	Unknown
BPES16	F	GB	Half-sisters II:1 and II:3 were affected; father I:2 was not affected, suggestive of germline mosaicism. II:1 had a premature birth (32 wk) with respiratory distress syndrome, intrauterine and postnatal growth retardation, microcephaly, moderate learning difficulties apparent from age 7 y, and strabismus; II:3 had normal psychomotor development	Microdel downstream of *FOXL2* (at 28.7 kb)	Normal	Two copies of *FOXL2*	Max. 188 kb (139959089–140147132)	*DB35–rs9834963* (38.27 kb)	*rs7627822–FOXL2* (28.7 kb)	Yes	Paternal

[a] F1 = familial, type I; F2 = familial, type II; F = familial, type undetermined; S = sporadic; S1 = sporadic, type I.
[b] AU = Australia; BE = Belgium; BY = Belarus; CA = Canada; CD = Congo; DK = Denmark; ES = Spain; FR = France; GB = Great Britain; KR = South Korea; NO = Norway; PL = Poland.
[c] FSH = follicle-stimulating hormone; IVF = in vitro fertilization; LH = luteinizing hormone; VSD = ventricle septum defect; y = year.
[d] del = deletion; incl. = including; Max. = at maximum.
[e] In parentheses is the length of the interval in which the centromeric and the telomeric breakpoints are located.

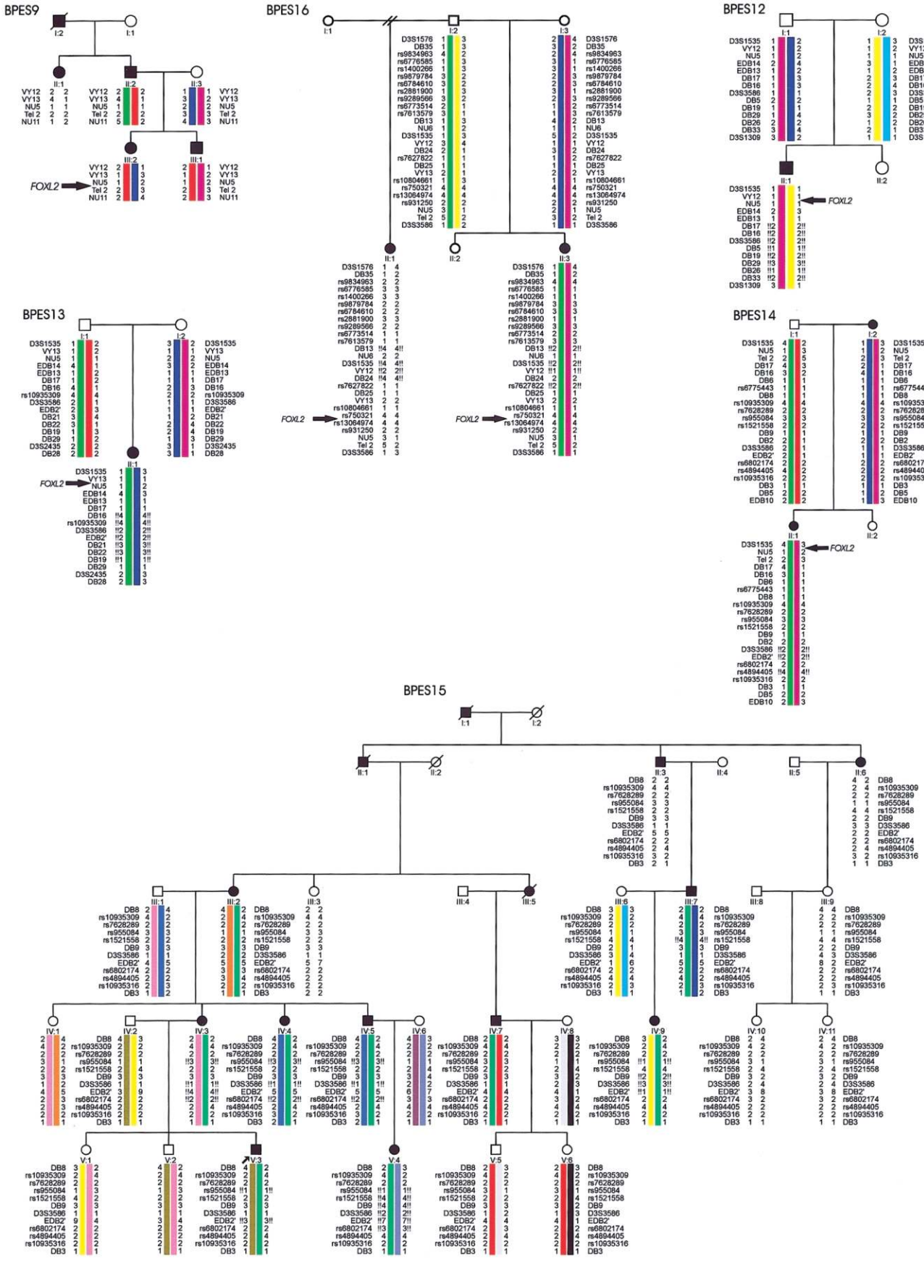
BPES9
BPES16
BPES12
BPES13
BPES14
BPES15
FOXL2

scopic deletions (in BPES1 and BPES3) (fig. 1*A* and table 2). In patient BPES11, MLPA analysis revealed a total *FOXL2* deletion; however, the extent could not be determined because of the lack of appropriate patient and parental material. The deletion breakpoints are scattered, suggesting lack of a deletion-prone region and nonhomologous end joining as the common causal mechanism (Shaw and Lupski 2004), which is supported by characterization of the junction fragment of an 8-kb deletion in family BPES9 with BPES type I (fig. 2 and fig. 3*C* and 3*D*). Attempts to characterize the junction fragments by long-range PCR failed for the other subtle deletions presented in this study.

In the three families with BPES in which several affected members are heterozygous for a total gene deletion (BPES9), a microdeletion (BPES7), or a submicroscopic deletion (BPES5), microsatellite analysis showed similar extents of the deletion in the affected family members of different generations, suggesting stability during meiosis (fig. 2 and fig. 4).

Previously, two submicroscopic deletions of >3.8 Mb and 3.2 Mb were found in patient BPES2 and the proband of BPES5, respectively, both of whom had psychomotor retardation and microcephaly as associated features. These findings led to a preliminary genotype-phenotype correlation (De Baere et al. 2001, 2003). Here, we identified a submicroscopic deletion of >3.5 Mb in a young woman with sporadic BPES (BPES4) who has microcephaly but apparently normal psychomotor development, suggesting that the extent of the deletion is not necessarily in linear correlation with the occurrence of developmental delay (table 2 and fig. 1*A*). In a recent study, it was postulated that mental retardation is associated with a heterozygous deletion of the Seckel-associated *ATR* gene located 3.6 Mb telomeric to *FOXL2* (Gille et al. 2003). In our series of patients, however, there was no consistent correlation between *ATR* haploinsufficiency and developmental delay, as seen in patient BPES4 and family BPES5 (table 2).

In addition, in 9 of 11 patients, the BPES type could not be determined (for prepubertal females or males with sporadic BPES). However, in the two families for which it was possible to assess the BPES type (BPES9 and BPES11), the deletion was found to lead to BPES and POF (type I), which is in agreement with previous genotype-phenotype correlations between heterozygous in-

The figure is available in its entirety in the online edition of *The American Journal of Human Genetics*.

Figure 3 Schematic diagram of *FOXL2* gene and protein, electropherogram of MLPA products, sequence electropherogram of the deletion junction fragment, and nucleotide sequence of the breakpoint junctions. The legend is available in its entirety in the online edition of *The American Journal of Human Genetics*.

Figure 2 Pedigrees with BPES and a rearrangement encompassing *FOXL2* or located outside of the transcription unit. Intragenic *FOXL2* mutations were excluded by sequencing of the ORF in all patients. MLPA was performed to assess changes in gene copy number, and haplotypes are based on microsatellite or SNP analysis. An exclamation mark (!) indicates hemizygosity of an allele. *BPES9,* Microsatellite analysis in two generations of this French family showed apparent linkage to *FOXL2*. However, no intragenic *FOXL2* mutation was found in affected members. MLPA analysis revealed a total gene deletion of *FOXL2*. Long-range PCR revealed the breakpoints of an 8-kb deletion (fig. 3). The occurrence of secondary amenorrhea in II:1 suggests this family has type I BPES. In addition, III:2 has a heart malformation in association with BPES. *BPES16,* In this family, two affected half-sisters (II:1 and II:3) have BPES, whereas their father (I:2) is clinically unaffected, suggesting germline mosaicism. FISH and microsatellite analysis revealed an extragenic deletion of 188 kb located 3′ of *FOXL2* in the half-sisters. Microsatellite analysis showed an apparent absence of this deletion in their father. However, quantitative studies revealed somatic mosaicism for this deletion in 5% of DNA from his leucocytes and 10% of DNA from his sperm cells, confirming germline mosaicism at the molecular level (table 3). *BPES12,* Upstream microdeletion in a 14-year-old male with sporadic BPES and additional features. MLPA showed normal *FOXL2* and *ATR* gene copy numbers, whereas several microsatellites at a distance from *FOXL2* were hemizygous, indicating a deletion outside of the transcription unit. The centromeric breakpoint of the deletion is located in a 69-kb interval between microsatellites *EDB14* and *DB17*; at the telomeric side, the deletion extends beyond the borders of the physical map in figure 1*A*, but does not contain *D3S1309*. The deletion encompasses at least several known and unknown genes (*LOC389152, BPESC1, MRPS22, COPB2, RBP2, ACTGP1, RBP1, NMNAT3,* and *CLSTN2*) and extends beyond 1.9 Mb. The contribution of each gene to the psychomotor retardation and other associated features in this patient is unclear. *BPES13,* Upstream microdeletion of maternal origin in a 2-year-old female with sporadic BPES who had normal psychomotor development and microcephaly. The deletion spans 567 kb at the most; the centromeric breakpoint is located between microsatellites *EDB14* and *DB16,* and the telomeric breakpoint is between markers *DB19* and *D3S2435*. The deletion covers part of *BPESC1, MRPS22, COPB2, RBP2, ACTGP1, RBP1,* and *NMNAT3*. *BPES14,* Microdeletion of ~200 kb 5′ of *FOXL2* in two affected females, I:2 and II:1, of a two-generation family with type II BPES. FISH analysis with probes RP11-548O1, RP11-306L14, RP11-319G6, Pac204O7, and Cos11L10 showed normal hybridization signals on both chromosomes 3, whereas RP11-657M13, Cos12P5, and Pac208L5 were deleted. One normal and one lighter signal were seen with RP11-219D15 and PAC169C10, confirming that the deletion breakpoints are located in these probes. The centromeric breakpoint of the deletion is located between *DB16* and *D3S3586,* and the telomeric breakpoint is between *EDB2*′ and *DB5*. *BPES15,* Extragenic microdeletion found in a five-generation Belgian family with BPES type II, previously linked to 3q23 (Messiaen et al. 1996). This 126-kb microdeletion is the smallest one upstream of *FOXL2* and delineates the SRO of the different microdeletions located at this side of *FOXL2* (detailed view in fig. 1*A*). FISH probes RP11-657M13 and PAC208L5 showed one lighter and one normal hybridization signal, thus indicating the borders of the deletion. Analysis with adjacent probes showed two normal signals. The hemizygous microsatellites indicate that the centromeric breakpoint is located between *rs10935309* and *rs955084* and the telomeric breakpoint is between *rs6802174* and *rs4894405* (fig. 1*A*).

The figure is available in its entirety in the online edition of *The American Journal of Human Genetics.*

Figure 4 Haplotypes of families BPES5 and BPES7, in which affected members carry a deletion encompassing *FOXL2*, illustrating the stability of deletions in the different generations. The legend is available in its entirety in the online edition of *The American Journal of Human Genetics.*

tragenic mutations leading to a *FOXL2* null allele and BPES type I (De Baere et al. 2003). Because of the small sample size, this hypothesis needs to be evaluated in additional studies of patients carrying (micro)deletions. To allow reliable genotype-phenotype correlations for psychomotor development and POF risk, an accurate delineation of deletions is a prerequisite.

In some informative families, it was possible to determine the parental origin of the deletion, but no parent-of-origin effect was observed (maternal:paternal deletion ratio was 4:3) (table 2). Thus, BPES does not belong to the group of conditions in which sex-dependent mechanisms may play a role in the origin of the underlying genomic rearrangement (e.g., Charcot-Marie Tooth 1A and hereditary neuropathy with liability to pressure palsies) (Lopes et al. 1997).

Genomic Rearrangements Outside of the Transcription Unit of FOXL2

A complex regulation of gene expression has been suggested for several forkhead transcription factors by the occurrence of chromosomal rearrangements (translocations) upstream (*FOXC1*) and downstream (*FOXC2*) of their respective transcription units (Davies et al. 1999; Fang et al. 2000). For the *FOXL2* locus, specifically, three translocation breakpoints located 170 kb upstream of the disease gene cause exactly the same phenotype as loss-of-function mutations (De Baere et al. 2000; Praphanphoj et al. 2000; Crisponi et al. 2001, 2004).

Here, we report five novel deletions mapping upstream and downstream of the transcription unit of *FOXL2* in patients with BPES with a phenotype identical to that caused by intragenic mutations. The presence of an intact transcription unit (coding sequence and copy number) was confirmed by sequencing and MLPA in all affected patients. The extragenic genomic rearrangements contribute to 5% (5/100) of all the molecular defects identified in our series of patients with BPES and are found in 14% (5/37) of our mutation-negative patients with BPES. They are found in patients with sporadic BPES and patients with familial BPES and are absent in unaffected individuals. An overview of the location and extent of these rearrangements is given in figure 1*A*, and relevant clinical data for the patients are given in table 2.

First, we identified a genomic rearrangement—presumed to be a microdeletion of ~188 kb—downstream of *FOXL2* in family BPES16, in which two affected half-sisters have typical BPES, whereas their father is clinically unaffected, which is suggestive of germline mosaicism (fig. 2 and table 2). To confirm paternal germline mosaicism at a molecular level, quantitative SNaPshot analysis was performed for three informative SNPs located in the deletion (*rs9879784, rs9289566,* and *rs6773514*) (table 3). We estimated that ~10% of the paternal germ cells and 5% of somatic peripheral blood lymphocytes carry the deletion (table 3). The estimated recurrence risk in this family is 10%, being significantly higher than the risk of a de novo event (<1%). This is the first case of germline mosaicism in BPES that is documented at the molecular level. This study indicates that this is an important issue to be considered in genetic counseling.

Second, we identified four overlapping microdeletions, which ranged from 126 kb to 1.9 Mb, upstream of the transcription unit of *FOXL2*. These extragenic deletions were found in two patients with a sporadic form of BPES (BPES12 and BPES13) and in two families (BPES14 and BPES15) (fig. 1*A* and fig. 2). In two of these families, assessment of the BPES type was possible; the absence of female infertility or overt POF in affected females of families BPES14 and BPES15 suggests that these 5′-located microdeletions do not significantly perturb ovarian expression of *FOXL2* and thus lead to BPES type II.

Of the two affected half-sisters in family BPES16 with the downstream microdeletion, II:3 has typical BPES with apparently normal psychomotor development at age 4 years, whereas II:1 has BPES and also presents moderate learning difficulties that were apparent from age 6 years, intrauterine and postnatal growth retardation, and microcephaly (fig. 2 and table 2). She was born at a gestational age of 32 weeks because of preeclampsia. There is no indication of a different extent of the deletion in the two patients. Another patient (BPES12), heterozygous for a 1.9-Mb upstream deletion, has BPES and presents additional features, including microcephaly, intrauterine and postnatal growth retardation, and a ventricular septum defect (fig. 2 and table 2). These additional features might represent a contiguous gene syndrome that can be explained by the extent

Table 3

Results of Quantitative SNaPshot Analysis with SNPs *rs6773514, rs9289566,* and *rs9879784*

The table is available in its entirety in the online edition of *The American Journal of Human Genetics.*

Table 4

Details of CNGs Found in the Respective SROs of the Upstream and Downstream Genomic Rearrangements

The table is available in its entirety in the online edition of *The American Journal of Human Genetics*.

of the deletion. In the other three families (BPES13, BPES14, and BPES15), no associated features were present. For the extragenic rearrangements, we can conclude that there is no association with psychomotor retardation and that there are as yet no arguments for a correlation with POF risk.

In familial cases BPES14, BPES15, and BPES16, microsatellite and FISH analysis indicated that the extent of the respective extragenic deletion is equal in each generation, suggesting stability during meiosis in these families (fig. 2). These clinical and molecular observations underscore the value of using complementary tools to delineate the extent of microdeletions together with assessment of the gene copy number of *FOXL2*.

The shortest region of deletion overlap (SRO) of the 5′ microdeletions involves a 126-kb region. Interestingly, it contains the human orthologue of the PIS locus in the goat. PIS, characterized by polledness (absence of horns) and XX intersexuality, is an animal model for BPES. Pailhoux et al. (2001) showed that it was caused by a 12-kb deletion located 280 kb upstream of *FOXL2*. This deletion does not contain any coding sequences and affects transcription of at least two genes in the PIS goat: the noncoding *PISRT1* and *FOXL2*, located at 20 kb and 280 kb from the deletion, respectively. It was suggested that the PIS locus contains elements involved in long-range *cis*-regulation of goat *FOXL2* (Pailhoux et al. 2001). Our current study lends further support to this hypothesis.

Moreover, this SRO is located telomeric to three known translocation breakpoints in BPES (fig. 1*A*). Crisponi et al. (2004) noted that these breakpoints are all located in intron 6 of the *MRPS22* gene. Using human-mouse comparative sequence analysis, they showed the presence of three highly conserved sequence blocks upstream of the most distal breakpoint, in introns 6, 11, and 12 of *MRPS22*. The PIS locus was shown to be located in the conserved sequence block in intron 11 of *MRPS22*. It was postulated that these conserved sequence blocks are candidate regions that might function as distant enhancers or have an influence on higher-order chromatin structure, both of which affect long-range *cis*-regulation of *FOXL2* expression.

CNGs in the SRO of Extragenic Rearrangements

Recent experimental approaches demonstrated that a fraction of CNGs in the genome act as *cis*-transcriptional regulators, although little is known about their function (Dermitzakis et al. 2002, 2003). Furthermore, it has been shown that conserved sequences are clustered around developmental genes and function as regulatory elements that affect embryonic development (Bejerano et al. 2004; Plessy et al. 2005). In addition, genomic variation in CNGs is presumed to be associated with phenotypic variability and even with human monogenic conditions (reviewed by Dermitzakis et al. [2005]). To identify potential CNGs, a comparative sequence analysis was undertaken in the SRO of the extragenic deletions. We made use of publicly available, gapped and ungapped alignments of the UCSC Genome Browser. Although a human-mouse alignment is generally used, we made a selection of conserved sequences across more distant species to enhance the functional significance of the selected CNGs. We performed human-chicken, human-pufferfish, human-zebrafish, and human-goat comparisons (the latter only for an available 48-kb goat sequence [GenBank accession number AF404302]). In the two regions of interest, we identified 25 putative CNGs common to human and chicken, pufferfish, and/or zebrafish and 1 common to human and goat. Seventeen of those were eventually selected as CNGs, after we filtered for coding and transposable elements (table 4). Some of them (CNG3–CNG5) are conserved up to pufferfish or zebrafish, strongly suggesting that they function as a regulatory element (table 4). CNG3–CNG7 are all contained in the human orthologue of the PIS locus. These CNGs were found to be located in the 9-kb conserved sequence block previously described by Crisponi et al. (2004).

Analysis of these sequences with a Transfac database revealed several interesting putative transcription-factor binding sites for FOXP3 in CNG5 and CNG9; for HNF-1 in CNG3, CNG9, CNG22, and CNG24; for HNF-4 in CNG1 and CNG2; and for embryonic gonadal regulator SOX9 in CNG3. Interestingly, a regulatory link between SOX9 and the PIS locus has already been suggested by Nikic and Vaiman (2004). We found that a binding site for FOXL1 (ATTCAATAAAGAAGTA), previously identified by Crisponi et al. (2004) in the 9-kb conserved sequence block, was situated in CNG3. The conserved nature of the elements located in the human orthologue of the PIS locus, together with the prediction of potentially relevant binding sites, provide arguments that they are *cis*-acting elements (e.g., an enhancer) regulating correct spatiotemporal *FOXL2* expression during embryonic development.

It is nearly impossible to obtain human samples that would allow meaningful analysis of regulation of *FOXL2* expression in developing eyelids and ovary. Such analysis currently relies on genotype-phenotype correlations of genomic rearrangements and BPES, comparative sequence analysis, and experimental validation—for instance, in animal models. In the two families in

which the BPES type could be assessed, BPES14 and BPES15, we found that the 5′ extragenic rearrangements led to BPES type II. This "mild" phenotype can be explained either (1) by a selective regulation of craniofacial *FOXL2* expression by the 5′ distant elements or (2) by regulation of both craniofacial and ovarian expression but with the absence of an ovarian phenotype in the case of a heterozygous deletion. The latter situation would be identical to the regulation of *FOXL2* expression in the goat, in which both the craniofacial and ovarian expression appear to be regulated by the PIS locus, but in which phenotypic expression of polledness and XX intersexuality depend on the heterozygous and homozygous states of the deletion, respectively.

There are other diseases known to be caused by genomic rearrangements lying at considerable distances from the disease gene and leading to phenotypes identical to those resulting from intragenic mutations. However, the majority is caused by chromosomal rearrangements (translocations), and only a minority results from deletions presumably affecting a regulatory element. The first reported example was that of the locus of control region (LCR) of the β-globin gene cluster. Translocation breakpoints and deletions in this conserved element cause autosomal recessive β-thalassemia due to silencing of the β-globin gene, which maps 50 kb downstream of the LCR (Driscoll et al. 1989). A hotspot for microdeletions has been identified, in patients with X-linked deafness type 3, that is 900 kb proximal to the *POU3F4* disease gene. The 8-kb SRO of these deletions contains a 2-kb sequence that is 80% conserved between human and mouse (de Kok et al. 1996). More recently, the autosomal recessive van Buchem disease was found to be caused by a homozygous deletion that is 52 kb downstream of the disease gene *SOST* and contains two CNGs (Balemans et al. 2002). Similarly, the upstream and downstream genomic rearrangements described here dissociate putative regulatory CNGs from their target gene *FOXL2* and lead to BPES, one of the first autosomal dominant conditions for which this mechanism has been demonstrated.

Our approach led to the identification of a molecular defect in 16 (43%) of 37 mutation-negative patients with BPES analyzed in this study. The lack of a sequence variation or a rearrangement in 21 patients, representing 17% (21/121) of the total patient group, might be explained by the fact that assessment of the four diagnostic criteria of BPES was done by different clinicians. In addition, the current strategy does not allow for detection of inversions and subtle extragenic rearrangements, such as deletions, duplications, and point mutations in regulatory elements. The latter mutational mechanism was demonstrated in autosomal dominant preaxial polydactyly syndrome in humans, for which four different pathogenic point mutations were found in a regulatory element of 750 bp named "ZRS," apparently regulating expression of *SHH* that maps 1 Mb away (Lettice et al. 2003).

General Conclusions

In summary, this is the first study, to our knowledge, to show that deletions mapping downstream and upstream of the *FOXL2* transcription unit cause BPES. Several potential upstream and downstream *cis*-acting regulatory elements were identified by delineation of these genomic rearrangements and by comparative genomics. The identification of the upstream deletions containing the human orthologue of the PIS locus in four patients with BPES provides evidence of human-goat conservation of the regulation of *FOXL2* expression and of the mutational mechanism. This study provides insight into the regulation of expression of *FOXL2,* one of the earliest markers of ovarian development. More generally, it contributes to the enlarging group of human developmental diseases caused by defective long-range regulation of gene expression. It further demonstrates one of the functions of conserved noncoding regions—that is, to act as a *cis*-regulatory element. Finally, our results emphasize that CNGs may be candidate regions for harboring genomic rearrangements in monogenic developmental disorders.

Acknowledgments

We thank the families with BPES for their cooperation. We acknowledge Sarah De Jaegere, Alicia Borderé, and Evelien Vanoverschelde, for their technical assistance. This study was supported by Bijzonder Onderzoeksfonds grant BOF2002/DRMAN/047 from Ghent University (to D.B.) and by the Fund for Scientific Research-Flanders grant 1.5.244.05 (to E.D.B.).

Web Resources

Accession numbers and URLs for data presented herein are as follows:

BACPAC Resources Center, http://bacpac.chori.org/
Biomax Human Genome Database, http://www.biomax.de/products/bhgdb/bhgdb.htm
ClustalW, http://www.ebi.ac.uk/clustalw/
Find Simple Repeats software, http://zeon.well.ox.ac.uk/git-bin/microsatellite.cgi
GenBank, http://www.ncbi.nlm.nih.gov/Genbank/ (for PIS locus [accession number AF404302] and 48-kb goat sequence [accession number AF404302])
International HapMap Project, http://www.hapmap.org/index.html.en
MRC-Holland, http://www.mrc-holland.com
mVista, http://genome.lbl.gov/vista/index.shtml
NCBI, http://www.ncbi.nlm.nih.gov/
Online Mendelian Inheritance in Man (OMIM), http://www.ncbi.nlm.nih.gov/Omim/ (for *FOXL2,* BPES, and IRID1)

RepeatMasker, http://www.repeatmasker.org/
UCSC Genome Browser, http://www.genome.ucsc.edu
The Wellcome Trust Sanger Institute, http://www.sanger.ac.uk/

References

Balemans W, Patel N, Ebeling M, Van Hul E, Wuyts W, Lacza C, Dioszegi M, Dikkers FG, Hildering P, Willems PJ, Verheij JB, Lindpaintner K, Vickery B, Foernzler D, Van Hul W (2002) Identification of a 52 kb deletion downstream of the *SOST* gene in patients with van Buchem disease. J Med Genet 39:91–97

Bejerano G, Pheasant M, Makunin I, Stephen S, Kent WJ, Mattick JS, Haussler D (2004) Ultraconserved elements in the human genome. Science 304:1321–1325

Bodega B, Porta C, Crosignani PG, Ginelli E, Marozzi A (2004) Mutations in the coding region of the *FOXL2* gene are not a major cause of idiopathic premature ovarian failure. Mol Hum Reprod 10:555–557

Cha SC, Jang YS, Lee JH, Kim HK, Kim SC, Kim S, Baek SH, Jung WS, Kim JR (2003) Mutational analysis of forkhead transcriptional factor 2 (*FOXL2*) in Korean patients with blepharophimosis-ptosis-epicanthus inversus syndrome. Clin Genet 64:485–490

Cocquet J, De Baere E, Gareil M, Pannetier M, Xia X, Fellous M, Veitia RA (2003) Structure, evolution and expression of the *FOXL2* transcription unit. Cytogenet Genome Res 101: 206–211

Cocquet J, Pailhoux E, Jaubert F, Servel N, Xia X, Pannetier M, De Baere E, Messiaen L, Cotinot C, Fellous M, Veitia RA (2002) Evolution and expression of *FOXL2*. J Med Genet 39:916–921

Crisponi L, Deiana M, Loi A, Chiappe F, Uda M, Amati P, Bisceglia L, Zelante L, Nagaraja R, Porcu S, Ristaldi MS, Marzella R, Rocchi M, Nicolino M, Lienhardt-Roussie A, Nivelon A, Verloes A, Schlessinger D, Gasparini P, Bonneau D, Cao A, Pilia G (2001) The putative forkhead transcription factor *FOXL2* is mutated in blepharophimosis/ptosis/epicanthus inversus syndrome. Nat Genet 27:159–166

Crisponi L, Uda M, Deiana M, Loi A, Nagaraja R, Chiappe F, Schlessinger D, Cao A, Pilia G (2004) *FOXL2* inactivation by a translocation 171 kb away: analysis of 500 kb of chromosome 3 for candidate long-range regulatory sequences. Genomics 83:757–764

Davies AF, Mirza G, Flinter F, Ragoussis J (1999) An interstitial deletion of 6p24-p25 proximal to the *FKHL7* locus and including *AP-2α* that affects anterior eye chamber development. J Med Genet 36:708–710

De Baere E, Beysen D, Oley C, Lorenz B, Cocquet J, De Sutter P, Devriendt K, Dixon M, Fellous M, Fryns JP, Garza A, Jonsrud C, Koivisto PA, Krause A, Leroy BP, Meire F, Plomp A, Van Maldergem L, De Paepe A, Veitia R, Messiaen L (2003) *FOXL2* and BPES: mutational hotspots, phenotypic variability, and revision of the genotype-phenotype correlation. Am J Hum Genet 72:478–487

De Baere E, Dixon MJ, Small KW, Jabs EW, Leroy BP, Devriendt K, Gillerot Y, et al (2001) Spectrum of *FOXL2* gene mutations in blepharophimosis-ptosis-epicanthus inversus (BPES) families demonstrates a genotype-phenotype correlation. Hum Mol Genet 10:1591–1600

De Baere E, Fukushima Y, Small K, Udar N, Van Camp G, Verhoeven K, Palotie A, De Paepe A, Messiaen L (2000) Identification of BPESC1, a novel gene disrupted by a balanced chromosomal translocation, t(3;4)(q23;p15.2), in a patient with BPES. Genomics 68:296–304

De Baere E, Lemercier B, Christin-Maitre S, Durval D, Messiaen L, Fellous M, Veitia R (2002) *FOXL2* mutation screening in a large panel of POF patients and XX males. J Med Genet 39:e43

De Baere E, Van Roy N, Speleman F, Fukushima Y, De Paepe A, Messiaen L (1999) Closing in on the BPES gene on 3q23: mapping of a de novo reciprocal translocation t(3;4)(q23;p15.2) breakpoint within a 45-kb cosmid and mapping of three candidate genes, *RBP1, RBP2,* and *β′-COP,* distal to the breakpoint. Genomics 57:70–78

de Kok YJ, Vossenaar ER, Cremers CW, Dahl N, Laporte J, Hu LJ, Lacombe D, Fischel-Ghodsian N, Friedman RA, Parnes LS, Thorpe P, Bitner-Glindzicz M, Pander HJ, Heilbronner H, Graveline J, den Dunnen JT, Brunner HG, Ropers HH, Cremers FP (1996) Identification of a hot spot for microdeletions in patients with X-linked deafness type 3 (DFN3) 900 kb proximal to the DFN3 gene *POU3F4*. Hum Mol Genet 5:1229–1235

Dermitzakis ET, Reymond A, Antonarakis SE (2005) Conserved non-genic sequences—an unexpected feature of mammalian genomes. Nat Rev Genet 6:151–157

Dermitzakis ET, Reymond A, Lyle R, Scamuffa N, Ucla C, Deutsch S, Stevenson BJ, Flegel V, Bucher P, Jongeneel CV, Antonarakis SE (2002) Numerous potentially functional but non-genic conserved sequences on human chromosome 21. Nature 420:578–582

Dermitzakis ET, Reymond A, Scamuffa N, Ucla C, Kirkness E, Rossier C, Antonarakis SE (2003) Evolutionary discrimination of mammalian conserved non-genic sequences (CNGs). Science 302:1033–1035

Driscoll MC, Dobkin CS, Alter BP (1989) $\gamma\delta\beta$-Thalassemia due to a *de novo* mutation deleting the 5′ β-globin gene activation-region hypersensitive sites. Proc Natl Acad Sci USA 86:7470–7474

Fang J, Dagenais SL, Erickson RP, Arlt MF, Glynn MW, Gorski JL, Seaver LH, Glover TW (2000) Mutations in *FOXC2* (MFH-1), a forkhead family transcription factor, are responsible for the hereditary lymphedema-distichiasis syndrome. Am J Hum Genet 67:1382–1388

Gille JJP, de Ru MH, Nieuwint AWM, van Hagen JM (2003) A patient with a genomic deletion encompassing *FOXL2* and *ATR*. Am J Hum Genet Suppl 73:287

Harris SE, Chand AL, Winship IM, Gersak K, Aittomaki K, Shelling AN (2002) Identification of novel mutations in *FOXL2* associated with premature ovarian failure. Mol Hum Reprod 8:729–733

Kleinjan DA, van Heyningen V (2005) Long-range control of gene expression: emerging mechanisms and disruption in disease. Am J Hum Genet 76:8–32

Lehmann OJ, Sowden JC, Carlsson P, Jordan T, Bhattacharya SS (2003) Fox's in development and disease. Trends Genet 19:339–344

Lettice LA, Heaney SJ, Purdie LA, Li L, de Beer P, Oostra BA,

Goode D, Elgar G, Hill RE, de Graaff E (2003) A long-range *Shh* enhancer regulates expression in the developing limb and fin and is associated with preaxial polydactyly. Hum Mol Genet 12:1725–1735

Lopes J, Vandenberghe A, Tardieu S, Ionasescu V, Levy N, Wood N, Tachi N, Bouche P, Latour P, Brice A, LeGuern E (1997) Sex-dependent rearrangements resulting in CMT1A and HNPP. Nat Genet 17:136–137

Mátyás G, Giunta C, Steinmann B, Hossle JP, Hellwig R (2002) Quantification of single nucleotide polymorphisms: a novel method that combines primer extension assay and capillary electrophoresis. Hum Mutat 19:58–68

Matys V, Fricke E, Geffers R, Gossling E, Haubrock M, Hehl R, Hornischer K, Karas D, Kel AE, Kel-Margoulis OV, Kloos DU, Land S, Lewicki-Potapov B, Michael H, Munch R, Reuter I, Rotert S, Saxel H, Scheer M, Thiele S, Wingender E (2003) TRANSFAC: transcriptional regulation, from patterns to profiles. Nucleic Acids Res 31:374–378

Messiaen L, Leroy BP, De Bie S, De Pauw K, Van Roy N, Speleman F, Van Camp G, De Paepe A (1996) Refined genetic and physical mapping of BPES type II. Eur J Hum Genet 4:34–38

Nikic S, Vaiman D (2004) Conserved patterns of gene expression in mice and goats in the vicinity of the polled intersex syndrome (PIS) locus. Chromosome Res 12:465–474

Pailhoux E, Vigier B, Chaffaux S, Servel N, Taourit S, Furet JP, Fellous M, Grosclaude F, Cribiu EP, Cotinot C, Vaiman D (2001) A 11.7-kb deletion triggers intersexuality and polledness in goats. Nat Genet 29:453–458

Plessy C, Dickmeis T, Chalmel F, Strahle U (2005) Enhancer sequence conservation between vertebrates is favoured in developmental regulator genes. Trends Genet 21:207–210

Praphanphoj V, Goodman BK, Thomas GH, Niel KM, Toomes C, Dixon MJ, Geraghty MT (2000) Molecular cytogenetic evaluation in a patient with a translocation (3;21) associated with blepharophimosis, ptosis, epicanthus inversus syndrome (BPES). Genomics 65:67–69

Schmidt D, Ovitt CE, Anlag K, Fehsenfeld S, Gredsted L, Treier AC, Treier M (2004) The murine winged-helix transcription factor *Foxl2* is required for granulosa cell differentiation and ovary maintenance. Development 131:933–942

Schouten JP, McElgunn CJ, Waaijer R, Zwijnenburg D, Diepvens F, Pals G (2002) Relative quantification of 40 nucleic acid sequences by multiplex ligation-dependent probe amplification. Nucleic Acids Res 30:e57

Schuelke M (2000) An economic method for the fluorescent labeling of PCR fragments. Nat Biotechnol 18:233–234

Shaw CJ, Lupski JR (2004) Implications of human genome architecture for rearrangement-based disorders: the genomic basis of disease. Hum Mol Genet Suppl 13:R57–R64

Uda M, Ottolenghi C, Crisponi L, Garcia JE, Deiana M, Kimber W, Forabosco A, Cao A, Schlessinger D, Pilia G (2004) *Foxl2* disruption causes mouse ovarian failure by pervasive blockage of follicle development. Hum Mol Genet 13:1171–1181

Udar N, Yellore V, Chalukya M, Yelchits S, Silva-Garcia R, Small K (2003) Comparative analysis of the *FOXL2* gene and characterization of mutations in BPES patients. Hum Mutat 22:222–228

Velagaleti GV, Bien-Willner GA, Northup JK, Lockhart LH, Hawkins JC, Jalal SM, Withers M, Lupski JR, Stankiewicz P (2005) Position effects due to chromosome breakpoints that map ~900 kb upstream and ~1.3 Mb downstream of *SOX9* in two patients with campomelic dysplasia. Am J Hum Genet 76:652–662

Zlotogora J, Sagi M, Cohen T (1983) The blepharophimosis, ptosis, and epicanthus inversus syndrome: delineation of two types. Am J Hum Genet 35:1020–1027